ISSN 2070-0482, Mathematical Models and Computer Simulations, 2017, Vol. 9, No. 3, pp. 390–403. © Pleiades Publishing, Ltd., 2017.

Spiking and Bursting of a Fractional Order of the Modified FitzHugh-Nagumo Neuron Model[1]

J. Alidousti* and R. Khoshsiar Ghaziani**

Department of Applied Mathematics, Shahrekord University, Shahrekord, Iran

**e-mail: javad.alidousti@stu.sku.ac.ir*

***e-mail: khoshsiar@sci.sku.ac.ir*

Received October 17, 2016

Abstract—This paper reports bursting behavior and related bifurcations in a fractional order FitzHugh-Nagumo neuron model, by adding sub fast-slow system. We classify different bursters of the system consisting fold/Hopf via a fold/fold hysteresis loop, homoclinic/homolininc cycle-cycle, fold/homoclinic, homoclinic/Hopf via homoclinic/fold hysteresis loop. We determine stability and dynamical behaviors of the equilibria of the system by numerical simulations.

Keywords: fractional order, bifurcation, FitzHugh-Nagumo model, fast-slow, bursting

DOI: 10.1134/S2070048217030036

1. INTRODUCTION

Neurons, the building blocks of the central nervous system, are highly complex dynamical systems. To understand the way neurons interact, simplified mathematical models are used, which aim to capture the essence of their underlying dynamics. Generic bifurcation models fall into this class of simplified neuron models. They aim to describe the underlying dynamics of the neuron by systems of ordinary differential equations. When these models are used in networks, techniques from the field of nonlinear dynamics can be applied to study phenomena of synchronization and pattern emergence. The essence of mathematical modeling is to find the right trade off between accuracy and simplicity. One of the most important questions in computational neuroscience is therefore which features of the complex dynamics observed in biological neurons form the essence of the specific tasks fulfilled by that neuron. Generic bifurcation models might provide a promising middle way between detailed models used by experimentalists and the more simple threshold and rate models used by computational neuroscientists.

Determining the dynamical behavior of an ensemble of coupled neurons is an important problem in computational neuroscience. The primary step for understanding this complex problem is to understand the dynamical behavior of individual neurons. Commonly used models for the study of individual neurons which display spiking/bursting behavior include, integrate-and-fire models and their variants [3, 4], FitzHugh-Nagumo model [5], Hindmarsh-Rose model [11]. Hodgkin-Huxley [7, 8] and Morris-Lecar model [19].

The FitzHugh-Nagumo neuron model is a mathematical abstraction for an excitable-oscillatory membrane, which is very adequate for emulation of small biological systems. The simplicity of the FitzHugh-Nagumo (FHN) model permits the entire solution to be viewed at once. This allows a geometrical explanation of important biological phenomena related to neuronal excitability and spike generating mechanism.

The relationship between spiking and bursting dynamics is a key question in neuroscience, particularly in understanding the origins of different neural coding strategies and the mechanisms of motor command generation and neural circuit coordination.

[1] The article is published in the original.

1.1. Bursting

Bursting behavior in neurons is a recurrent transition between a quiescent state and repetitive spiking (state of repetitive firing), see [11, 12, 25]. Many mathematical models of bursters often can be written in the singularly perturbed form

$$\begin{cases} \dot{x} = f(x,y) \quad (\text{fast spiking}), \\ \dot{y} = \mu g(x,y) \quad (\text{slow modulation}), \end{cases} \tag{1}$$

where $x \in \mathbb{R}^m$ is a vector of fast variables responsible for repetitive firing. It accounts, e.g., for the membrane voltage and fast ion channels, activation and inactivation gating variables for fast currents. The vector $y \in \mathbb{R}^k$ is a vector of slow variables that modulates the firing. It accounts for slow ion channels and currents. (e.g., gating variable of a slow K^+ current, an intracellular concentration of Ca^+ ions, etc.). Small parameter $\mu \ll 1$ is a ratio of fast/slow time scales. We say that the burster is of the $m + k$ type when the fast subsystem is m- dimensional and the slow subsystem is k-dimensional.

First, let us consider the fast subsystem $\dot{x} = f(x; y)$ alone and treat y as a bifurcation parameter. This is a standard approach known as dissection of bursting (Rinzel and Lee (1987)). As y changes slowly, the attractors of the fast subsystem bifurcate. The bifurcation of equilibrium that corresponds to transition from rest state to repetitive firing which determines how the repetitive firing appears, is named burster. A partial classification of bursters based on these bifurcations is provided by Wang and Rinzel (1995), Bertram et al. (1995), and Hoppensteadt and Izhikevich (1997). A complete classification is provided by Izhikevich (2000). For example, when both bifurcations are saddle-node on limit cycle, the burster is said to be parabolic. When the rest activity disappears via saddle-node bifurcation and the repetitive firing disappears via a saddle separatrix loop bifurcation, the burster is said to be of square-wave type. When the quiescent state loses stability via an Andronov-Hopf bifurcation and repetitive firing disappears via a double limit cycle bifurcation or another Andronov-Hopf bifurcation, the burster is said to be elliptic. A distinctive feature of elliptic bursting is that the frequency of emerging and ceasing spiking is nonzero, while the amplitude may be small. Since Andronov-Hopf bifurcation may be subcritical or supercritical, there are many subtypes of elliptic bursters. An elliptic burster is said to be supercritical or Hopf/Hopf when both Andronov-Hopf bifurcations are supercritical (Izhikevich (1998)). An elliptic burster is said to be subcritical or sub Hopf/fold cycle when the rest activity loses stability via subcritical Andronov-Hopf bifurcation, and the repetitive firing disappears via a double limit cycle bifurcation (also known as saddle node of limit cycles or fold of limit cycles). Since there is a coexistence state of rest and limit cycle attractors, the periodic transition between them often occurs via a hysteresis loop.

1.2. Classification of Bursters

Bursting is usually caused by a slow voltage- or calcium-dependent process that can modulate fast spiking activity. We refer to a burster as being a point-cycle when the quiescent state is an equilibrium point and the spiking state is a limit cycle. When the quiescent state is a small amplitude (sub threshold) oscillation, then the burster is said to be a cycle-cycle. We refer to a burster as being planar when the fast spiking subsystem is two-dimensional. A complete classification of all 16 planar point- cycle bursters, though without the naming scheme, was first provided by Hoppensteadt and Izhikevich (1997). Among them were the well-known

- Fold/homoclinic burster, also known as square-wave or Type I burster.
- Circle/circle burster, also known as parabolic or Type II burster.
- Sub Hopf/fold cycle burster, also known as elliptic or Type III burster.
- Fold/fold cycle burster, also known as Type IV burster.
- Fold/Hopf burster, also known as tapered or Type V burster.
- Fold/circle burster, also known as triangular burster.

The paper is organized as follows: In Section 2, we present some basic materials on neuroscience and fractional calculus and introduced the classical FitzHugh-Nagumo model. Fractional FitzHugh-Nagumo model and detailed analysis on the stability of the equilibria is carried out in Section 3. In Section 4, we perform numerical simulations of the system by computing different orbits of the classical and fractional system and discussion. In Section 5, we conclude the paper.

2. THE CLASSICAL FITZHUGH-NAGUMO NEURON MODELS

In this paper we consider an autonomous differential equation introduced in [11], which is a version of Bonhoeffer-van der Pol model or FitzHugh-Nagumo (FHN) model, as follows:

$$\begin{cases} \dot{x} = x - \dfrac{x^3}{3} - y + I, \\ \dot{y} = \varepsilon(a + x - S(y)), \\ \dot{z} = \mu x, \end{cases} \tag{2}$$

where

$$S(y) = \frac{b}{1 + e^{\frac{c-y}{d}}}.$$

This model is a multi-time-scale system characterized by two fast variables x, y and a slow adaptation current z. Here x mimics the membrane voltage and the recovery variable y mimics activation of an outward current. The parameter I mimics the injected current, the parameters b and c describe the kinetics of the recovery variable y and μ recovery variable z. For sake of simplicity we assume $I = 0$. Then we investigate dynamics of fractional order of the FHN model.

2.1. A Brief Overview of Fractional Calculus

Fractional calculus is a generalization of classical differentiation and integration to arbitrary order. In recent years, fractional calculus has been a fruitful field of research in science and engineering. Also a varieties of schemes for numerical solution of fractional differential equations are proposed [1, 14, 15]. Meanwhile, applications of fractional differential equations to physics, biology and engineering are a recent focus of interests [6, 13].

Two types of fractional derivatives of Riemann-Liouville and Caputo derivatives, have been often used in fractional differential systems. We briefly recall these definitions.

Definition 1. *The Riemann-Liouville integral $J_{t_0}^{\alpha}$ with fractional order $\alpha \in (0,\infty)$ of function $x(t)$ is defined as:*

$$J_{t_0}^{0} x(t) := \frac{1}{\Gamma(\alpha)} \int_{t_0}^{t} (t-\tau)^{\alpha-1} x(\tau)\, d\tau,$$

Where $\Gamma(.)$ is the gamma function. For $\alpha = 0$ we set $J_{t_0}^{0} := Id$, the identity operator.

Definition 2. *The Riemann-Liouville derivative with fractional order $\alpha \in \mathbb{R}_+$ of function $x(t)$ is defined by:*

$${}_{RL} D_{t_0}^{\alpha} x(t) := \frac{d^m}{dt^m} J_{t_0}^{m-\alpha} x(t),$$

where $m = \lceil \alpha \rceil := \min\{k \in \mathbb{Z} : k \geq \alpha\}$, is the ceiling of α.

Definition 3. *The Caputo derivative with fractional order $\alpha \in \mathbb{R}^+$ of function $x(t)$ is defined by:*

$${}_{C} D_{t_0}^{\alpha} x(t) := J_{t_0}^{m-\alpha} \frac{d^m}{dt^m} x(t)$$

where $m = \lceil \alpha \rceil$.

We use the following theorem to investigate the stability of the fractional-order model :

Theorem 1. *[20]*

Consider the following fractional-order system:

$$\frac{d^{\alpha} x}{dt^{\alpha}} = f(x), \quad x(0) = x_0$$

with $\alpha \in (0, 1)$ *and* $x \in \mathbb{R}^n$. *The equilibrium points of the above system are solutions to the equation* $f(x) = 0$. *An equilibrium is asymptotically stable if all eigenvalues* λ_j *of the Jacobian matrix* $J = \frac{\partial f}{\partial x}$ *evaluated at the equilibrium satisfy* $|\arg(\lambda_i)| > \frac{\alpha\pi}{2}, i = 1, 2, \ldots, n$.

2.2. Advantages of Using the Fractional-Order Capacitor of Order $0 < \alpha < 1$ in Neuron Dynamics

As pointed out in [16, 24, 26], from the basic electrical formula, the current I is the first-order derivative, the constant capacitance C and the voltage V, it holds

$$I = C\frac{dV}{dt},$$

with the following relationship

$$I = C\frac{d^{\alpha}V}{dt^{\alpha}}, \quad 0 < \alpha < 1, \tag{3}$$

that represents a normal capacitive behavior, reflecting the property of real dielectrics and insulators. Without loss of generality, assume that a step voltage $V_0u(t)$ is applied at $t = 0$. By applying the Laplace transform and inverse Laplace transform to both sides of above equations respectively, one has [24, 26]

$$I(t) = CV_0\delta(t), \tag{4}$$

and

$$I(t) = \frac{CV_0}{\Gamma(1-\alpha)}t^{-\alpha}, \quad 0 < \alpha < 1, \tag{5}$$

where $\delta(t)$ is the Dirac delta function. In the latter case, the current follows the power law, and it decays as a rate $t^{-\alpha}$ continuously with time, unlike the case defined by Eq. (4) for which the current jumps to 0 at any time $t > 0$. A number of electric simulation experiments verify the correctness of the power law with different values of α, for example $\alpha = .76$ for warm fog sciatic neuron and $\alpha = .86$ for cold fog sciatic neuron [16, 24]. For the limit case: $\alpha \to 1$, Eq. (5) is consistent with Eq. (4) due to $\frac{1}{\Gamma(1-\alpha)} \to 0, \alpha \to 1$. When $0 < \alpha < 1$, Eq. (5) not only shows the power law, but also reflects the memory property of membrane of the neuron, because the current described by Eq. (3) over $[0, t]$
equals to

$$\frac{d^{\alpha}V}{dt^{\alpha}} = \frac{1}{\Gamma(1-\alpha)}\int_0^t (t-\tau)^{-\alpha}V'(\tau)\,d\tau = \frac{V_0}{\Gamma(1-\alpha)}\int_0^t (t-\tau)^{-\alpha}\delta(\tau)\,d\tau = \frac{V_0}{\Gamma(1-\alpha)}t^{-\alpha},$$

Hence, it is reasonable to use a fractional-order capacitor with order $0 < \alpha < 1$ in modeling of neuron dynamics.

3. FRACTIONAL-ORDER FITZHUGH-NAGUMO MODEL AND ITS STABILITY

We introduce the fractional order system of FHN by replacing the usual integer order derivatives by fractional order Caputo-type derivatives in a modified FitzHugh-Nagumo neuron model introduced in [11] to obtain the following fractional order FitzHugh-Nagumo neuron model (FFHN):

$$\begin{cases} \frac{d^{\alpha}x}{dt^{\alpha}} = x - \frac{x^3}{3} - y + I, \\ \frac{d^{\alpha}y}{dt^{\alpha}} = \varepsilon(a + x - S(y)), \\ \frac{d^{\alpha}z}{dt^{\alpha}} = \mu x, \end{cases} \tag{6}$$

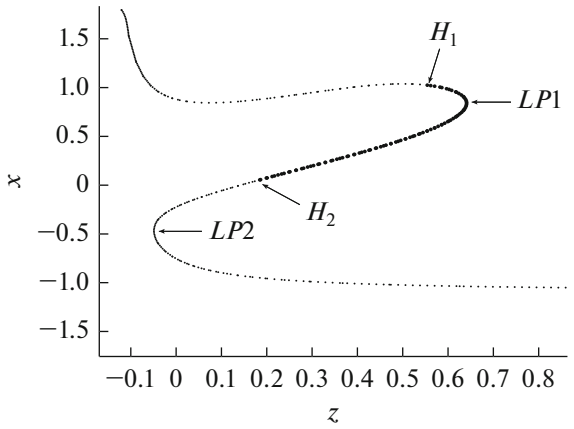

Fig. 1. Steady state of fast subsystem (6) in (z, x) space for $\alpha = 0.9$.

where

$$S(y) = \frac{b}{1 + e^{\frac{c-y}{d}}}.$$

The fractional order system (6) is more suitable than that of the integer order system due to memory effects.

First, we decompose the model into fast and slow subsystems, and then analyze the dynamics of the full system in the limit of the slow variable treated as a bifurcation parameter. The full system can be decomposed into a fast subsystem

$$\begin{cases} \dfrac{d^{\alpha}x}{dt^{\alpha}} = x - \dfrac{x^3}{3} - y + I, \\ \dfrac{d^{\alpha}y}{dt^{\alpha}} = \varepsilon(a + x - S(y)), \end{cases}$$

and different slow subsystems, for instance, $\dfrac{d^{\alpha}z}{dt^{\alpha}} = \mu x$. By treating z as a slow variable, also as a bifurcation parameter, the steady state of fast subsystem is given by:

$$\begin{cases} x - \dfrac{x^3}{3} - y = 0, \\ \varepsilon\left(a + x - \dfrac{b}{1 + e^{\frac{c-y}{d}}}\right) = 0, \end{cases}$$

or

$$\begin{cases} F(x, y) = 0, \\ G(x, y) = 0, \end{cases}$$

In these models, fast series of spikes burst over oscillations of the slow variable.

However, the behavior of fast and slow dynamics are clearly correlated and it can be observed that high values of the slow variable correspond with spikes of the fast variable and low values of the slow variable correspond with resting periods of the fast variable.

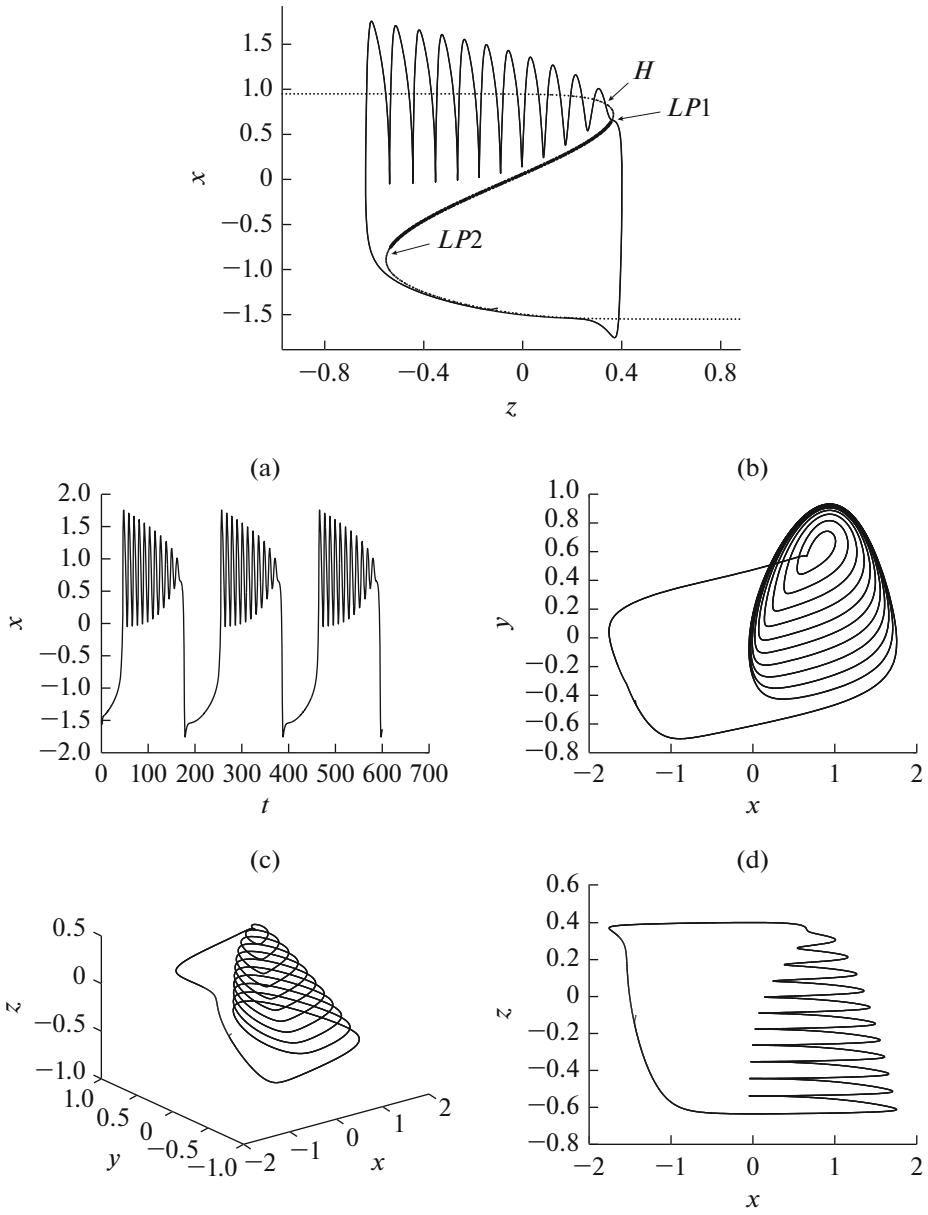

Fig. 2. Bifurcation diagram of the system (6), respect to the slow variable z. Fold/Hopf bursting via fold/fold hysteresis loop, The rest state disappears via fold bifurcation, and the repetitive spiking disappears via supercritical Hopf bifurcation. Simulations of (6), (a), (b), (c), (d), with slow subsystem $\frac{d^{\alpha}z}{dt^{\alpha}} = \mu x$ when $\alpha = 1$, $a = 1.55$, $c(z) = z$, $b = 2.5$, $d = 0.1$, $\varepsilon = 0.5$, $\mu = 0.01$.

For each equilibrium $E_* = (x^*, y^*)$, let A be the Jacobian matrix evaluated at the E_*, i.e.,

$$A = J\big|_{E_*} = \begin{pmatrix} \dfrac{\partial F}{\partial x} & \dfrac{\partial F}{\partial y} \\ \dfrac{\partial G}{\partial x} & \dfrac{\partial F}{\partial y} \end{pmatrix}_{E_*} . \tag{7}$$

By Theorem (1), we check the stability of equilibria An equilibrium is asymptotically stable if all eigenvalues λ_i of the Jacobian matrix A satisfy $|\arg(\lambda_i)| > \dfrac{\alpha\pi}{2}$, $i = 1, 2$, and an equilibrium is unstable if there is

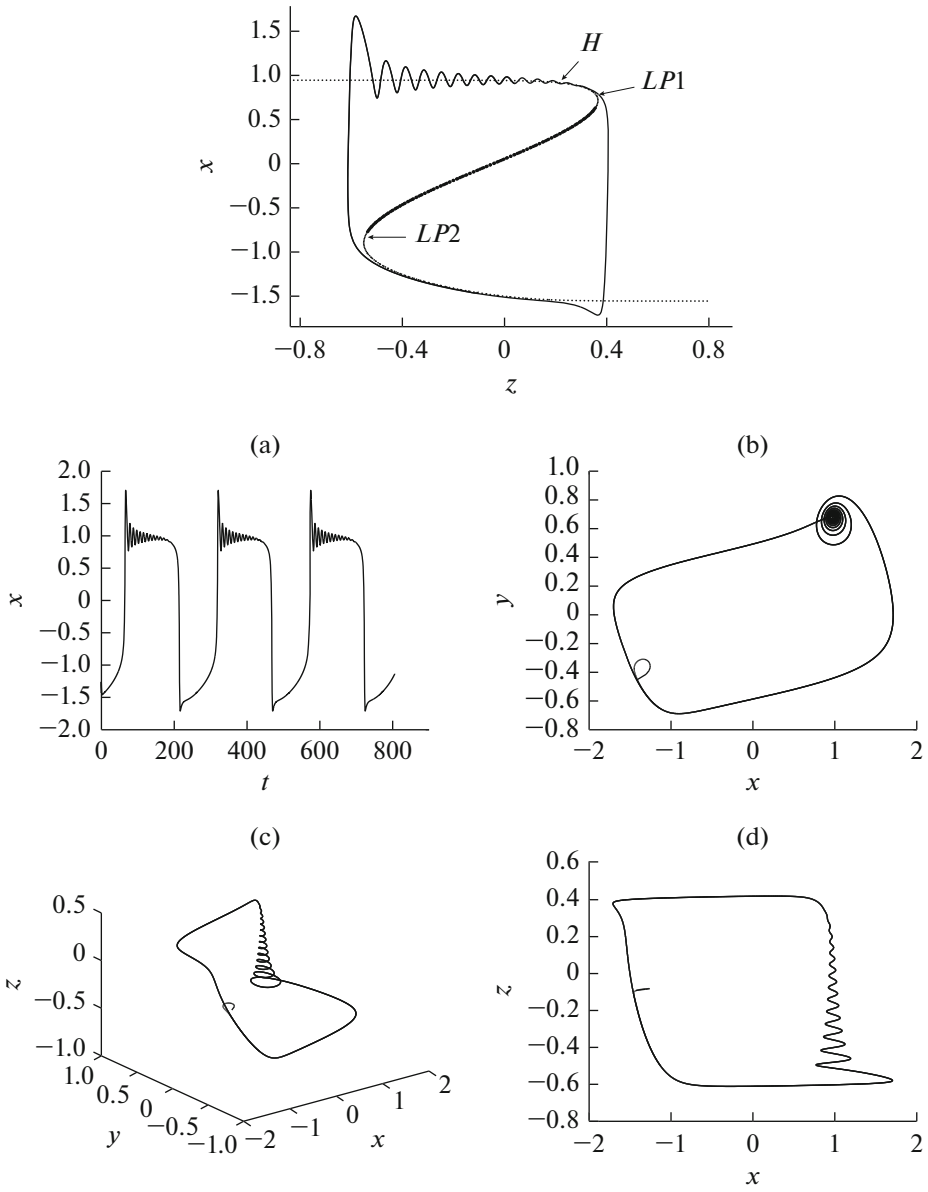

Fig. 3. Bifurcation diagram of the system (6), respect to the slow variable z. Fold/Hopf bursting via fold/fold hysteresis loop, The quiescent state disappears via a fold bifurcation, and the repetitive spiking disappears via a supercritical Hopf bifurcation. Simulations of (6), (a), (b), (c), (d), with slow subsystem $\frac{d^{\alpha}z}{dt^{\alpha}} = \mu x$ when $\alpha = 0.9$, $a = 1.55$, $c(z) = z$, $b = 2.5$, $d = 0.1$, $\varepsilon = 0.5$, $\mu = 0.01$.

some λ_i satisfying $|\arg(\lambda_i)| < \frac{\alpha\pi}{2}$. A Hopf bifurcation occurs if all of the eigenvalues satisfy in $|\arg(\lambda_i)| > \frac{\alpha\pi}{2}$ except for a pair of conjugate eigenvalues with $|\arg(\lambda_i)| = \frac{\alpha\pi}{2}$.

A bifurcation diagram of fast subsystem with respect to the slow variable z is shown in Fig 1. It is clear that there exists a Z-shaped equilibria bifurcation curve in the (z, x)-plane which is made up of three branches:

• On the upper branch (pallid line), the equilibrium is unstable (at least one eigenvalue with absolute argument less than $\left|\frac{\alpha\pi}{2}\right|$), its stability changes via a Hopf bifurcation indicated by H_1, in which absolute value of argument of the corresponding eigenvalues equals to $\left|\frac{\alpha\pi}{2}\right|$.

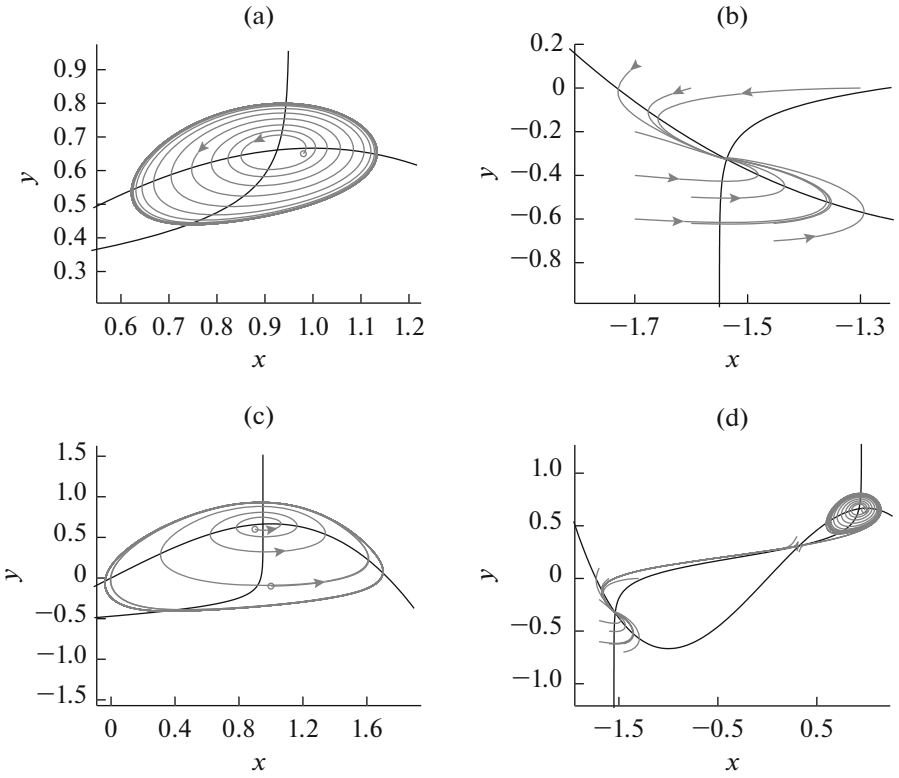

Fig. 4. The phase trajectory of model (6) in (x, y)-plane with different parameters (a) $z = -0.52$, (b) $z = 0.2$, (c) $z = 0.35$, (d) $z = 0.2$.

• The middle branch (bold line) is made up of stable points (absolute of argument of all the eigenvalues are greater than $\left|\frac{\alpha\pi}{2}\right|$). Stability on this branch changes via a Hopf bifurcation indicated by H_2.The points $LP1$ and $LP2$ represent fold bifurcations of equilibrium.

• On the lower branch, the equilibria are all unstable.

4. NUMERICAL SIMULATION AND DISCUSSIONS

In this section, numerical simulation is carried out to locate the bursting patterns of the fractional FitzHugh-Nagumo model, including new patterns that did not observe in the corresponding integer-order model. The parameter values that are used for the classical FitzHugh-Nagumo model with fast-slow variables are taken from [11].

We use the numerical approach introduced in [18], which approximates derivatives of f as:

$$\left.\frac{d^{\alpha}f(t)}{dt^{\alpha}}\right|_{t_k=kh} = h^{-\alpha}\sum_{j=0}^{h}(-1)^{j}\binom{\alpha}{j}f(kh-jh), \quad k = 0,1,2,\ldots$$

Using this approximation, with zero initial conditions for the following system:

$$\frac{d^{\alpha}x(t)}{dt^{\alpha}} = F(t,x(t),y(t),z(t)),$$

$$\frac{d^{\alpha}y(t)}{dt^{\alpha}} = G(t,x(t),y(t),z(t)),$$

$$\frac{d^{\alpha}z(t)}{dt^{\alpha}} = H(t,x(t),y(t),z(t)),$$

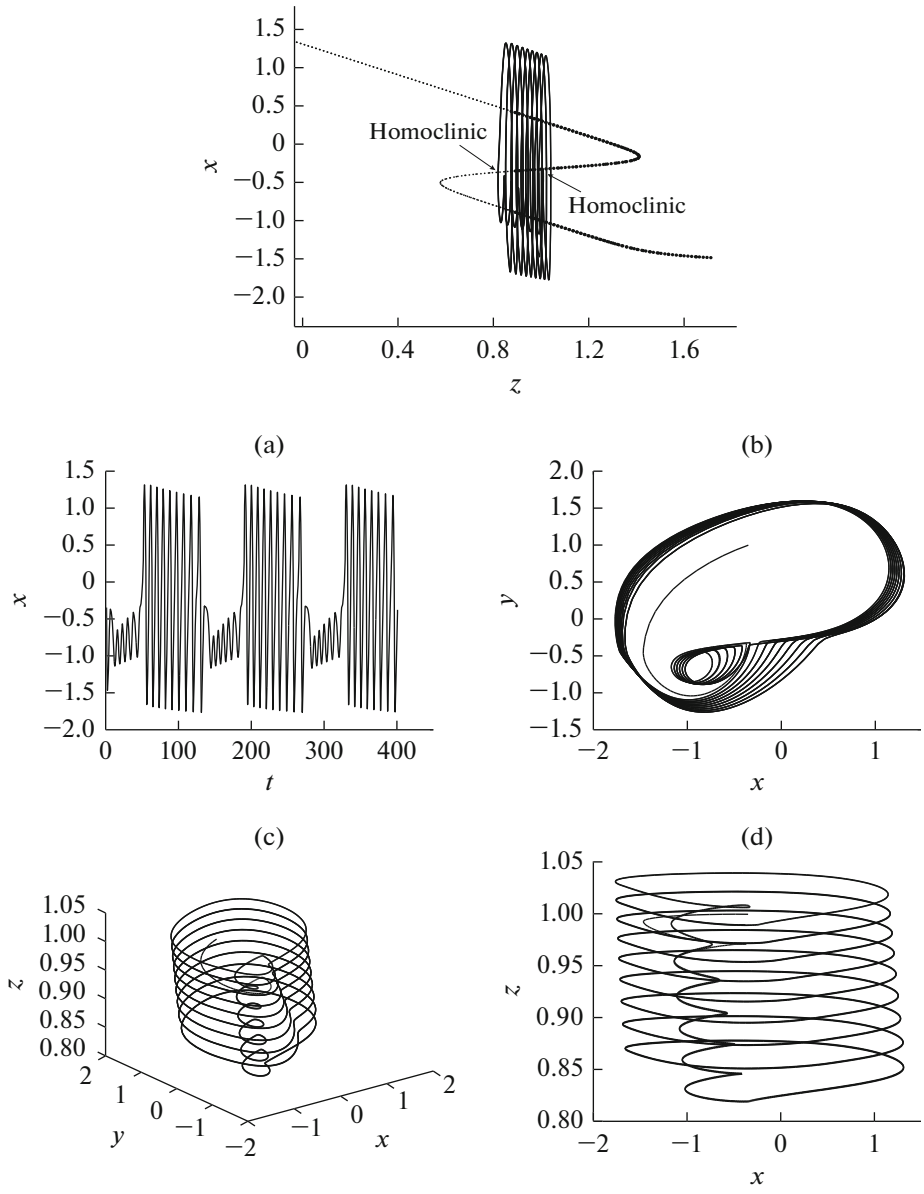

Fig. 5. Bifurcation diagram of the system (6), the same fast subsystem and different slow subsystem, respect to the slow variable z. Homoclinic/homoclinic cycle-cycle bursting: The transitions between quiescent and spiking limit cycles occur via saddle homoclinic orbit bifurcations. Simulations of (6), (a), (b), (c), (d), with different slow subsystem $\frac{d^{\alpha}z}{dt^{\alpha}} = \mu(0.4 + x)$ when $\alpha = 1$, $a = 1.3$, $a(z) = z$, $c = -0.32$, $d = 0.05$, $\varepsilon = 1$, $\mu = 0.01$.

lead to

$$\sum_{j=0}^{k}(-1)^{j}\binom{\alpha}{j}x(t_{k-j}) = h^{\alpha}F(t_k, x(t_k), y(t_k), z(t_k)),$$

$$\sum_{j=0}^{k}(-1)^{j}\binom{\alpha}{j}y(t_{k-j}) = h^{\alpha}G(t_k, x(t_k), y(t_k), z(t_k)),$$

$$\sum_{j=0}^{k}(-1)^{j}\binom{\alpha}{j}z(t_{k-j}) = h^{\alpha}H(t_k, x(t_k), y(t_k), z(t_k)),$$

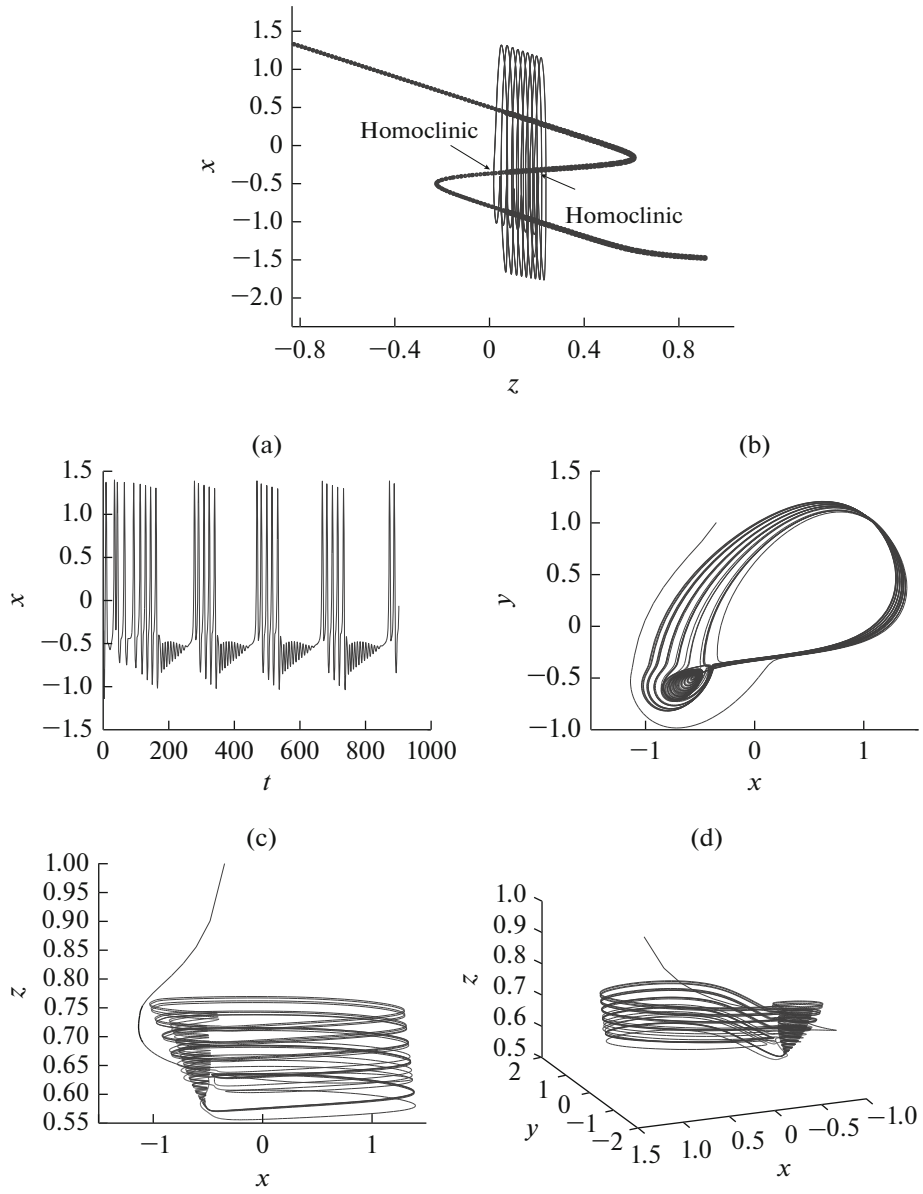

Fig. 6. Bifurcation diagram of the system (6), the same fast subsystem and different slow subsystem, respect to the slow variable z. Homoclinic/homoclinic cycle-cycle bursting: The transitions between quiescent and spiking limit cycles occur via saddle homoclinic orbit bifurcations. Simulations of (6), (a), (b), (c), (d), with different slow subsystem $\frac{d^{\alpha}z}{dt^{\alpha}} = \mu(0.4 + x)$ when $\alpha = 0.9$, $a = 1.3$, $a(z) = z$, $c = -0.32$, $d = 0.05$, $\varepsilon = 1$, $\mu = 0.01$.

where $t_k = kh, x_k = x(t_k)$. For the sake of simplicity, we set $w_j^{(\alpha)} = (-1)^j \binom{\alpha}{j}, j = 0,1,\ldots$ to obtain the following recurrence relation:

$$w_0^{(\alpha)} = 1, \quad w_k^{(\alpha)} = \left(1 - \frac{\alpha + 1}{k}\right) w_{k-1}^{(\alpha)}, \quad k = 1,2,\ldots$$

It turns out that show that the fractional-order derivative plays an important role to activate the slow ion channel faster.

To figure out differences between bifurcation scenarios of classical and fractional models, for the same parameter values, we compare numerical results obtained for the integer order system with that of frac-

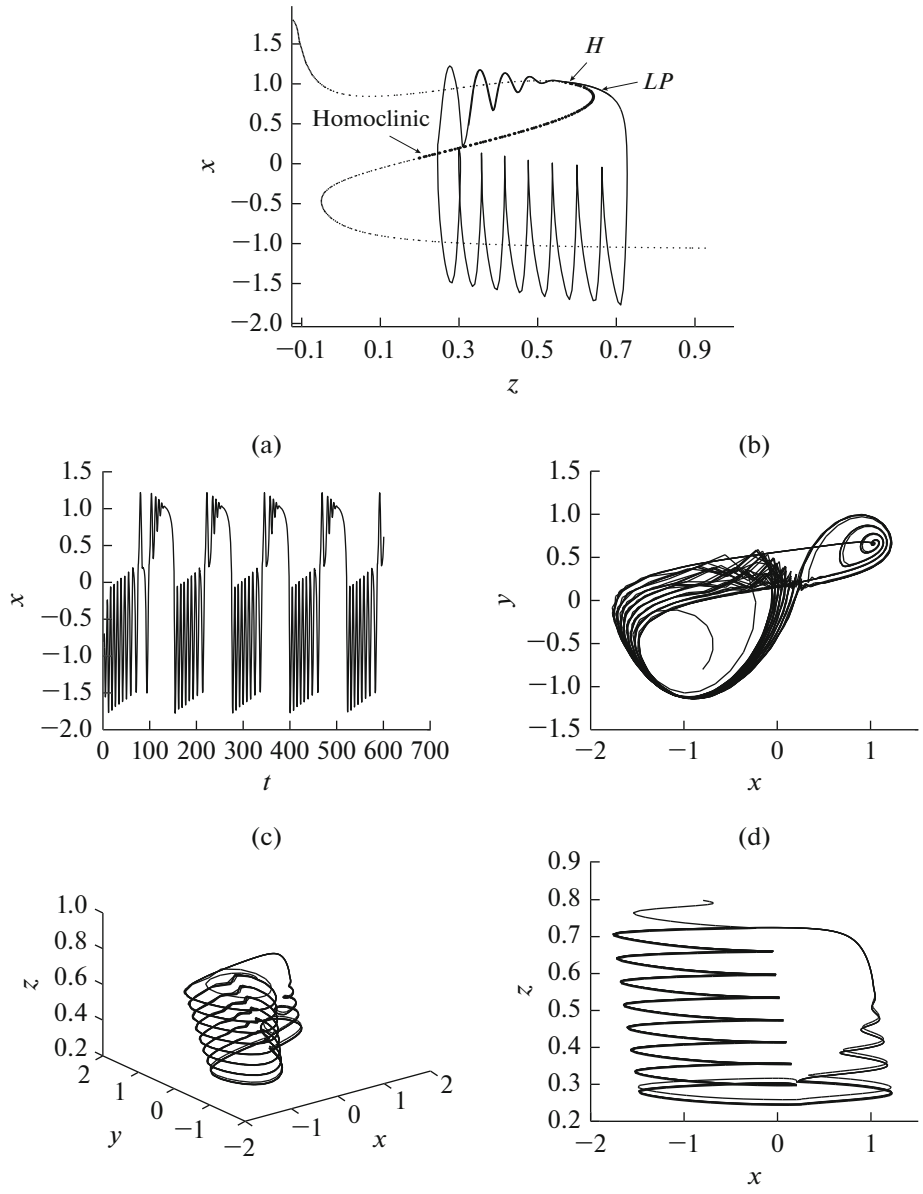

Fig. 7. Bifurcation diagram of the system (6), the same fast subsystem and different slow subsystem, respect to the slow variable z. Homoclinic/Hopf cycle-cycle bursting via homoclinic/fold hysteresis loop: The quiescent oscillation disappears via saddle homoclinic orbit bifurcation and the periodic spiking disappears via supercritical Hopf bifurcation.. Simulations of (6), (a), (b), (c), (d), with different slow subsystem $\frac{d^{\alpha}z}{dt^{\alpha}} = \mu x$ when $\alpha = 1$, $a(z) = 0.77 + \frac{0.33z}{z + 0.15}$, $b(z) = 1.65 + z$, $c = -0.15 + z$, $d = 0.1$, $\varepsilon = 1$, $\mu = 0.01$.

tional order system. We particularly compare Fig. 2 with Figs. 3, Fig. 5 with Figs. 6, Fig. 7 with Fig. 8, to examine different bifurcation scenarios for classical and fractional systems, respectively, for the same parameter values with different α. We set $\alpha = 1$ and $\alpha = 0.9$, for the classical and fractional systems respectively. Figures 2 and 3, different perspective of same picture, show the time history of a fold/Hopf bursting via fold/fold hysteresis loop, for a Hopf bifurcation H. The fast variable x forms a cycle of relaxation oscillation process in (z, x)-plane with respect to slow variable z. As the current value z decreases, the unstable node on the lower branch coincides with the stable node on the middle branch, the fold bifurcation occurs at $LP2$, meanwhile, a stable limit cycle appears around the unstable focus on the upper branch due to a Hopf bifurcation. Hence, the lower rest state switches to the upper repetitive spiking state, as z increases, stability of the equilibria on the upper branch changes via a supercritical Hopf bifurcation and then the

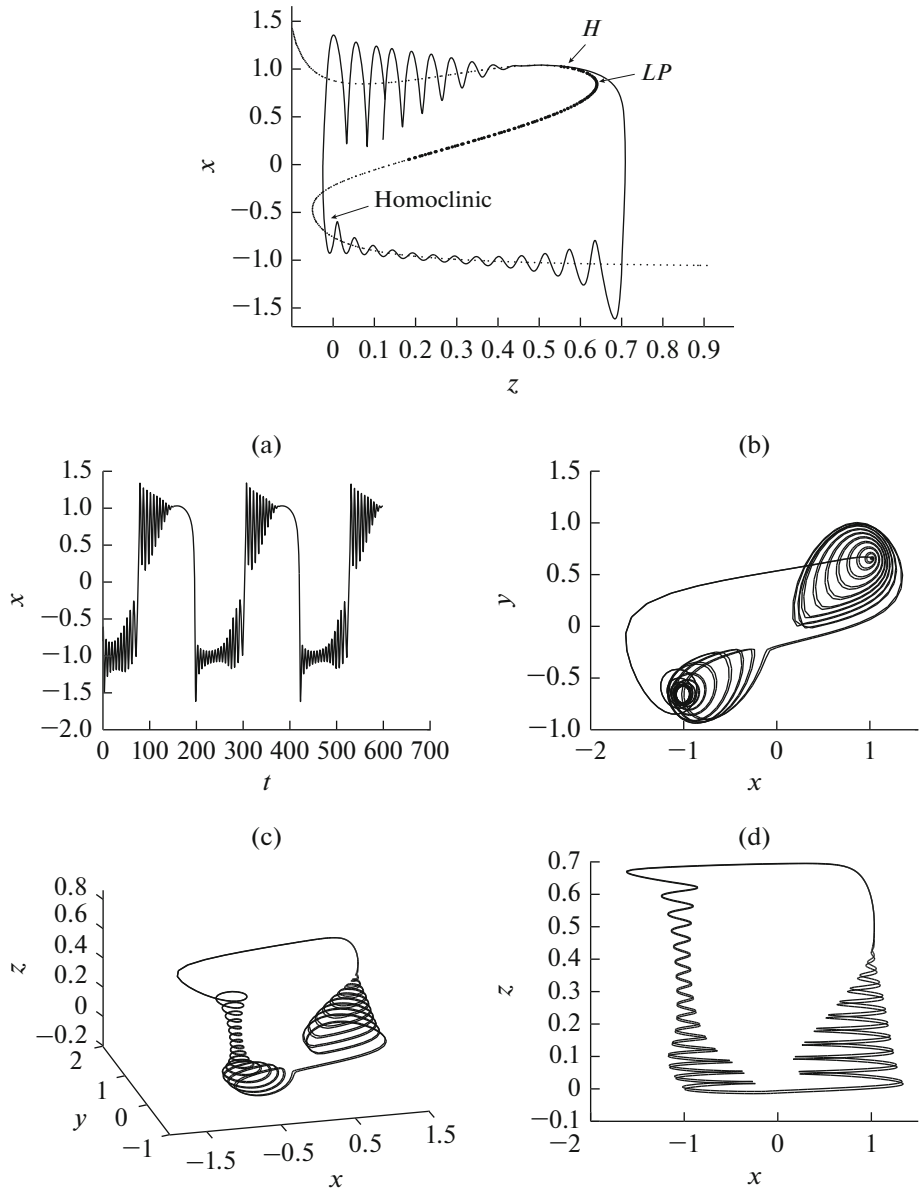

Fig. 8. Bifurcation diagram of the system (6), the same fast subsystem and different slow subsystem, respect to the slow variable z. Homoclinic/Hopf cycle-cycle bursting via homoclinic/fold hysteresis loop: The quiescent oscillation disappears via saddle homoclinic orbit bifurcation and the periodic spiking disappears via supercritical Hopf bifurcation. Simulations of (6), (a), (b), (c), (d), with different slow subsystem $\frac{d^{\alpha}z}{dt^{\alpha}} = \mu x$ when $\alpha = 0.9$, $a(z) = 0.77 + \frac{0.33z}{z + 0.15}$, $b(z) = 1.65 + z$, $c = -0.15 + z$, $d = 0.1$, $\varepsilon = 1$, $\mu = 0.01$.

stable limit cycle converges to a upper stable focus crossing the Hopf point H. So the upper repetitive spiking state is back to the rest state on the upper branch. Eventually, as z increases further the other fold bifurcation at $LP1$ relevant to transition from the upper rest state to the lower rest state to form a close cycle of relaxation oscillation.

In short, the whole relaxation oscillation process of this type of bursting contains four bifurcation points: the transition between the lower rest state and the upper repetitive spiking state which is relevant to a fold/ Hopf bifurcation at $LP2$ and a H, respectively, the other two critical bifurcation points relevant to transition between the upper state and the lower state are a fold/fold bifurcation at $LP1$ and a $LP2$, respectively, which form a hysteresis loop. Hence, according to the classification by Izhikevich, this type

of bursting is known as fold/(supercritical) Hopf bursting via fold/fold hysteresis loop. Further, if the critical points of bifurcation at the H and $LP1$ coincide, then the hysteresis loop disappears.

When $\alpha = .9$, bursting types are shown in Fig. 3. We can see that the slow ion channel is activated faster by the fractional-order derivative, i.e., the equilibrium potential varies in a smaller range, compared with that of the integer-order case.

The phase portrait of system (6) with different values of z, Fig. 4, enhances our understanding of the bifurcation mechanism corresponding to such bursting type. Figure 4 corresponds to the case of Fig. 3. In Fig. 4a there exists a stable limit cycle which emerges around the upper unstable equilibrium. In Fig. 4d a stable and two unstable equilibria are indicated, the stable equilibrium is the same one as indicated in (b). In (c) a stable equilibrium is shown which coexists with a stable limit cycle.

Scenarios corresponding to the Figs. 5, 6, 7, 8 can be treated similarly.

5. CONCLUDING REMARKS

In this paper, by numerical means, we analyze bursting behaviors and corresponding bifurcation scenarios of a fractional order FitzHugh-Nagumo neuron model. For this purpose, we add a sub fast-slow system to the fractional model and by numerical simulation we classify different bursters, namely, fold/Hopf via a fold/fold hysteresis loop, homoclinic/homolininc cycle-cycle, fold/homoclinic, homoclinic/Hopf via homoclinic/fold hysteresis loop.

REFERENCES

1. K. Diethelm, *The Analysis of Fractional Differential Equations* (Springer, Berlin, Heidelberg, 2010).
2. A. I. Ehibilik, R. M. Borisyuk, and D. Roose, "Numerical bifurcation analysis of a model of coupled neural oscillators," Int. Ser. Numer. Math. **104**, 215–228 (1992).
3. G. B. Ermentrout and N. Kopell, "Parabolic bursting in an excitable system coupled with a slow oscillation," SIAM J. Appl. Math. **46**, 233–253 (1986).
4. G. B. Ermentrout, "Type I membranes, phase resetting curves and synchrony," Neural Comput. **8**, 979–1001 (1996).
5. R. Fitzhugh, "Impulses and physiological states in models of nerve membrane," Biophys. J. **1**, 445–466 (1961).
6. R. Hifer, *Application of Fractional Calculus in Physics* (World Scientific, Singapore, 2000).
7. A. L. Hodgkin and A. F. Huxley, "A quantitative description of membrane current and application to conduction and excitation in nerve," J. Physiol. **117**, 500–544 (1954).
8. A. L. Hodgkin, "The local changes associated with repetitive action in a non-modulated axon," J. Physiol. **107**, 165–181 (1948).
9. F. C. Hoppensteadt and E. M. Izhikevich, *Weakly Connected Neural Networks* (Springer, New York, 1997).
10. E. M. Izhikevich, "Class 1 neural excitability, conventional synapses, weakly confornected networks and mathematical foundations of pulse coupled models," IEEE Trans. Neural Networks **10**, 499–507 (1999).
11. E. M. Izhikevich, "Neural excitability, spiking and bursting," Int. J. Bifurcat. Chaos **10**, 1171–1266 (2000).
12. E. M. Izhikevich, "Subcritical elliptic bursting of bautin type," SIAM J. Appl. Math. **60**, 503–535 (2000).
13. A. A. Kilbas, H. M. Srivastava, and J. J. Trujilo, *Theory and Applications of Fractional Differential Equations* (Elsevier, Amsterdam, 2006).
14. P. Kumar and O. P. Agrawal, "An approximate method for numerical solution of fractional differential equations," Signal Proccess. **6**, 2602–2610 (2006).
15. C. P. Li and Y. H. Wang, "Numerical algorithm based on Adomian decomposition for fractional differential equations," Comput. Math. Appl. **57**, 1627–1681 (2009).
16. R. L. Magin, "Fractional calculus in bioengineering," Crit. Rev. Biomed. Eng. **32**, 1–104 (2004).
17. D. Mishra, A. Yadav, and P. K. Kalra, "Chaotic behavior in neural network and FitzHugh-Nagumo neuronal model," Lect. Notes Comput. Sci. **3316**, 868–873 (2004).
18. C. A. Monje, Y. Q. Chen, B. M. Vinagre, D. Y. Xue, and V. Feliu, *Fractional Order Systems and Controls: Fundamentals and Applications* (Berlin, Springer, 2010).
19. C. Morris and H. Lecar, "Voltage oscillations in the Barnacle giant muscle fiber," J. Biophys. **35**, 193–213 (1981).
20. I. Petras, *Fractional-Order Nonlinear Systems: Modeling, Analysis and Simulation* (Springer, London, Beijing, 2011).
21. J. Rinzel, "Models in neurobiology," in *Nonlinear Phenomena in Physics and Biology* (Plenum, New York, 1981), pp. 345–367.

22. J. Rinzel and G. B. Ermentrout, "Analysis of neural excitability and oscillations," in *Methods in Neuronal Modeling* (MIT, Cambridge, MA, 1989).
23. J. Rinzel, "A formal classification of bursting mechanisms in excitable systems," Lect. Notes Biomath. **71**, 267–281 (1987).
24. M. Shi and Z. Wang, "Abundant bursting patterns of a fractional-order Morris-Lecar neuron model," Commun. Nonlin. Sci. Numer. Simulat. **19**, 1956–1969 (2014).
25. H. Wang and Q. Wang, "Bursting oscillations, bifurcation and synchronization in neuronal systems," Chaos, Solitons, Fractals **44**, 667–675 (2011).
26. S. Westerlund and L. Ekstam, "Capacitor theory," IEEE Trans. Dielectr. Electr. Insul. **1** (8), 26–39 (1994).